ACTA PHYSIOLOGICA

Acta Physiol 2014, 211, 161–175

# Slc26a3 deficiency is associated with loss of colonic $HCO_3^-$ secretion, absence of a firm mucus layer and barrier impairment in mice

**F. Xiao,[1,2,*] Q. Yu,[1,2,*] J. Li,[1,3,*] M. E. V. Johansson,[4,*] A. K. Singh,[1] W. Xia,[1,5] B. Riederer,[1] R. Engelhardt,[1] M. Montrose,[6] M. Soleimani,[6] D. A Tian,[2] G. Xu,[3] G. C. Hansson[4] and U. Seidler[1]**

*1 Department of Gastroenterology, Hannover Medical School, Hannover, Germany*

*2 Department of Gastroenterology, Tongji Hospital, Huazhong University of Science & Technology, Wuhan, China*

*3 Department of Nephrology, Tongji Hospital, Huazhong University of Science & Technology, Wuhan, China*

*4 Department of Medical Biochemistry, University of Gothenburg, Gothenburg, Sweden*

*5 School of Medicine, Key Lab of Combined Multiorgan Transplantation, The First Affiliated Hospital, Zhejiang University, Hangzhou, China*

*6 Center on Genetics of Transport and Epithelial Biology, University of Cincinnati, Cincinnati, OH, USA*

Received 5 September 2013,
revision requested 8 November 2013,
revision received 16 December 2013,
accepted 17 December 2013
Correspondence: U. Seidler, Hannover Medical School, Department of Gastroenterology, Carl-Neuberg-Str. 1, 30625 Hannover, Germany.
E-mail: seidler.ursula@mh-hannover.de

*These authors have equally contributed.

## Abstract

**Aim:** Downregulated in adenoma (DRA, Slc26a3) is a member of the solute carrier family 26 (SLC26), family of anion transporters, which is mutated in familial chloride-losing diarrhoea (CLD). Besides $Cl^-$-rich diarrhoea, CLD patients also have a higher-than-average incidence of intestinal inflammation. In a search for potential explanations for this clinical finding, we investigated colonic electrolyte transport, the mucus layer and susceptibility against dextran sodium sulphate (DSS)-induced colitis in $Slc26a3^{-/-}$ mice.

**Methods:** $HCO_3^-$ secretory ($J_{HCO3^-}$) and fluid absorptive rates were measured by single-pass perfusion *in vivo* and in isolated mid-distal colonic mucosa in Ussing chambers *in vitro*. Colonocyte intracellular pH ($pH_i$) was assessed fluorometrically, the mucus layer by immunohistochemistry and colitis susceptibility by the addition of DSS to the drinking water.

**Results:** $HCO_3^-$ secretory ($J_{HCO3-}$) and fluid absorptive rates were strongly reduced in $Slc26a3^{-/-}$ mice compared to wild-type (WT) littermates. Despite an increase in sodium/hydrogen exchanger 3 (NHE3) mRNA and protein expression, and intact acid-activation of NHE3, the high colonocyte pH in $Slc26a3^{-/-}$ mice prevented $Na^+/H^+$ exchange-mediated fluid absorption *in vivo*. Mucin 2 (MUC2) immunohistochemistry revealed the absence of a firm mucus layer, implying that alkaline secretion and/or an absorptive flux may be necessary for optimal mucus gel formation. $Slc26a3^{-/-}$ mice were highly susceptible to DSS damage.

**Conclusions:** Deletion of DRA results in severely reduced colonic $HCO_3^-$ secretory rate, a loss of colonic fluid absorption, a lack of a firmly adherent mucus layer and a severely reduced colonic mucosal resistance to DSS damage. These data provide potential pathophysiological explanations for the increased susceptibility of CLD patients to intestinal inflammation.

*Keywords* anion exchanger, bicarbonate, chloride-losing diarrhoea, intestinal barrier, mucin, sodium/hydrogen exchanger.

 doi: 10.1111/apha.12220 

Familial chloride-losing diarrhoea (CLD) is an autosomal recessive inherited disorder with high prevalence in Eastern Finland (Hihnala *et al.* 2006, Wedenoja *et al.* 2010, 2011). Patients with CLD have mutations in the downregulated in adenoma (DRA) (Slc26a3) gene (Wedenoja *et al.* 2011). DRA (Slc26a3) is a member of the Slc26 anion transporter gene family. Recent investigations demonstrated the high expression of this gene (Talbot & Lytle 2010, Xiao *et al.* 2012a) in the mid-distal colon, where it absorbs $Cl^-$ in exchange for $HCO_3^-$. In conjunction with $Na^+/H^+$ exchangers and the epithelial $Na^+$ channel ENaC, DRA activity will result in net NaCl and fluid absorption. Accordingly, the Slc26a3$^{-/-}$ mouse mimics features of CLD in displaying an increase in stool water as well as in stool $Cl^-$ content (Schweinfest *et al.* 2006). The mice die early, with rare survivors older than 4–5 months of age. CLD patients survive into adulthood with appropriate lifelong electrolyte and fluid substitution (Hihnala *et al.* 2006, Wedenoja *et al.* 2010, 2011). CLD complications have been studied in the Finnish cohort and include a higher-than-normal incidence of acute as well as chronic intestinal inflammation (Wedenoja *et al.* 2010), including an increased incidence of inflammatory bowel disease (IBD)-like manifestations (Hihnala *et al.* 2006, Wedenoja *et al.* 2010). Slc26a3 was identified as a susceptibility gene for ulcerative colitis in a Japanese genome-wide association study (Asano *et al.* 2009). A pathophysiological explanation for the increased susceptibility of CLD patients to intestinal inflammation is currently missing.

Luminal alkalinization rates in the colon are largely dependent on the presence of luminal $Cl^-$, probably due to DRA-mediated $Cl^-/HCO_3^-$ exchange (Xiao *et al.* 2012a,b). A role of DRA in duodenal and caecal $HCO_3^-$ secretion has already been documented (Walker *et al.* 2009, Alper *et al.* 2011). A relationship between $HCO_3^-$ secretion and mucus gel properties has been suggested (Garcia *et al.* 2009), as well as a relationship between an intact colonic mucus layer and epithelial health (Johansson *et al.* 2010a,b). The mucus layer is particularly prominent in the mid-distal colon, where DRA is also expressed most strongly. We therefore speculated that CLD patients may have low mid-distal colonic $HCO_3^-$ secretion rates and that this may interfere with mucus layer formation. The Slc26a3$^{-/-}$ mouse was used as a CLD model, and mid-distal colonic $HCO_3^-$ secretion and fluid absorption were measured in anaesthetized mice *in vivo* and *in vitro*. We also assessed the mucus layer quality immunohistochemically and studied the protective barrier properties of the colon by subjecting the mice to a dextran sodium sulphate (DSS) challenge. Our data provide the first description of pathophysiological fluid and $HCO_3^-$ transport and alterations in the firmly adherent mucus layer in the colonic mucosa of Slc26a3-deficient mice.

## Materials and methods

### Animals

The Slc26a3$^{-/-}$ mouse strain (Schweinfest *et al.* 2006) and the Slc9a3$^{-/-}$ mouse strain (Schultheis *et al.* 1998) were bred at Hannover Medical School under standard temperature and light conditions, and the conditions of breeding have been recently described (Xia *et al.* 2013). WT mice received the diet prior to the experiments, where they were cohoused with the knock-out (KO) littermates, but not all the time, because of weight gain on that diet. The mice were age- and sex-matched and used between 10 and 16 weeks of age. All experiments involving animals were approved by the Hannover Medical School Committee on investigations involving animals and an independent committee assembled by the local authorities.

### Blood gas analysis of Slc26a3$^{-/-}$ and Slc26a3$^{+/+}$ mice

Mice were anaesthetized by isoflurane and arterial blood was drawn from a carotid catheter and immediately analysed in a blood gas analyser (Radiometer, Copenhagen, Denmark). Alternatively, mice were killed by cervical dislocation, and immediately, blood was drawn by direct heart puncture and analysed.

### pH-stat titration of $HCO_3^-$ secretory rates in isolated mid-distal colonic mucosa

Ussing chamber experiments were performed to measure $HCO_3^-$ secretion *in vitro* as described previously (Tuo *et al.* 2006, Xiao *et al.* 2012a,b) in the open voltage mode with intermittent current pulses (100 $\mu$Amp every 60 s) to record the electrical resistance and calculate a nominal short-circuit current ($I_{sc}$). For the epithelial sodium channel (ENaC) current measurement, the mucosa was short-circuited with identical solutions in either chamber (Xiao *et al.* 2012a). For the Ussing chamber studies, the 'mid-distal' part of the colonic mucosa was used. This is the 3–4 cm proximal to the very distal (last 1 cm) part of the colon (which lies extraperitoneally within the anal canal). More technical information is in the supplementary file.

### $HCO_3^-$ secretion in the mid-distal colon of Slc26a3$^{-/-}$ and Slc26a3$^{+/+}$ mice in vivo

The measurement of $HCO_3^-$ secretion was performed by single-pass perfusion, as described previously (Xiao

 

*et al.* 2012a,b). The perfused colonic segment started 3–4 cm distal to the caecocolonic junction and ended approx. 1 cm before the anus, and it is designated as 'mid-distal colon' in the text. It largely overlaps the part that we used for Ussing chamber studies. More technical information is in the supplementary file.

### *Isolation of colonic crypts*

Intact colonic crypts were isolated from inverted mid-colonic segments (2 cm distal to the caecocolonic junction to 1 cm proximal to the anal canal) by a $Ca^{2+}$ chelation method exactly as previously described (Cinar *et al.* 2007).

### *Steady-state $pH_i$ measurements and acid-activated NHE3 activity measurements*

Steady-state $pH_i$ was assessed by measuring BCECF fluorescence in the different regions of the colonic crypt for 20 min during stable conditions, then performing a calibration in a very narrow pH range (in which the steady-state $pH_i$ is expected), as described (Hegyi *et al.* 2004). Acid-activated sodium/hydrogen exchanger 3 (NHE3) activity was measured as $Na^+$-dependent, Hoe642-insensitive, S1611-sensitive proton flux, as previously described (Bachmann *et al.* 2004, Cinar *et al.* 2007), except that two successive and identical ammonium prepulses were performed, and 20 $\mu$M S1611 was added to the $Na^+$-containing perfusate after the second ammonium pulse, in which $pH_i$- recovery took place. The buffer composition, as well as a representative $pH_i$ trace to demonstrate the experimental protocol, is given in the supplementary file. For technical explanation, see also the legend to Figure 3.

### *Quantitative PCR protocol*

RNA isolation as well as the PCR followed published protocols (Broere *et al.* 2009), with further details given in the supplementary file.

### *Histology and immunostaining*

Tissues were fixed in 4% paraformaldehyde (PFA), and paraffin-embedded sections were stained with haematoxylin and eosin (HE). In order to identify the mucus layer, distal colon was excised from Slc26a3$^{-/-}$ and WT mice immediately after killing and fixed in Carnoy fixative (Johansson *et al.* 2008). Paraffin-embedded sections were stained for mucin with Alcian blue/periodic acid-Schiff (PAS) or by Muc2-directed immunohistochemistry as previously described (Johansson *et al.* 2008). NHE3 immunostaining was performed exactly as previously described, and care was taken to image the WT and KO sections at identical settings of the confocal microscope (Lin *et al.* 2010).

### *Susceptibility of the Slc26a3$^{-/-}$ mice to DSS-induced colitis*

The establishment of the acute DSS colitis model for this particular type of mouse geno- and phenotype is described in the supplementary file and demonstrated in Figure S1. Because we noted the marked susceptibility of the Slc26a3$^{-/-}$ mice to DSS colitis in pilot experiments, we subjected control mice to 6, 4 and 2% DSS for 7 days (Figure S1). Slc26a3$^{-/-}$ mice were subjected to 2% DSS in the experiment shown in this paper. Histological analysis of colitis severity was assessed by leucocyte infiltrates, mucosal ulcerations, crypt deformities, goblet cell depletion, erosions, enlargement of the lymphoid aggregates and signs of submucosal thickening. More technical information is in the supplementary file.

### *Agents*

Tetrodotoxin was purchased from Biotrend Chemicals AG (Wengen, Switzerland). Forskolin was purchased from Alexis Biochemicals (Lörrach, Germany). Other reagents were purchased from Sigma–Aldrich (Deisenhofen, Germany).

### *Statistics*

All results were expressed as the mean ± SE. The data were analysed by ANOVA with Tukey's post hoc analysis for multiple comparisons or Student's t-tests for paired samples. $P < 0.05$ was considered statistically significant.

## Results

### *Slc26a3$^{-/-}$ mice display metabolic alkalosis with respiratory compensation*

Blood gas analysis of Slc26a3$^{-/-}$ and Slc26a3$^{+/+}$ mice showed that the absence of DRA resulted in a slightly but significantly more alkaline blood pH, which is partly compensated by $CO_2$ retention (Table S1). When mice were studied for their fluid absorptive and $HCO_3^-$ secretory rates under anaesthesia, these differences were compensated for by different solutions infused intra-arterially via a carotid catheter (less or no $HCO_3^-$ in the Slc26a3$^{-/-}$ mice), and no significant differences were seen in the blood gas analysis between Slc26a3$^{-/-}$ and Slc26a3$^{+/+}$ mice, as published previously (Singh *et al.* 2010).

 

### *Strong reduction in basal $HCO_3^-$ secretory rate in mid-distal colonic mucosa of Slc26a3$^{-/-}$ mice* in vitro

$HCO_3^-$ output rates ($J_{HCO3}^-$) into the luminal bath were quantified in mid-distal colonic mucosa from Slc26a3$^{-/-}$ and Slc26a3$^{+/+}$ mice. $J_{HCO3}^-$ was high and further increased by forskolin in WT mid-distal colonic mucosa (Fig. 1a). A striking decrease in basal $J_{HCO3}^-$ and no significant stimulation of $\Delta J_{HCO3}^-$ by forskolin (FSK) were seen in mid-distal colonic mucosa of Slc26a3$^{-/-}$ mice (Fig. 1a). The calculated basal $I_{sc}$ was more negative in the Slc26a3$^{-/-}$ mid-distal colon (Fig. 1b) and it increased less strongly after FSK addition compared to WT mucosa. The tissue resistance was not different between Slc26a3$^{-/-}$ and Slc26a3$^{+/+}$ mice and decreased after FSK stimulation in both genotypes (Fig. 1c). Because the decrease in tissue resistance $R_t$ upon FSK stimulation in murine mid-distal colon is largely, but not completely, inhibited by deletion of cystic fibrosis transmembrane regulator (CFTR) (Xiao *et al.* 2012b), the CFTR-independent decrease is probably due to BK channel ZERO splice variant activation with ensuing $K^+$ secretion (Sørensen *et al.* 2010). Under voltage clamp conditions (equal ionic composition and $CO_2/O_2$ gassing on both sides), the basal $I_{sc}$ was lower and the difference in $I_{sc}$ between Slc26a3$^{-/-}$ and Slc26a3$^{+/+}$ was amiloride

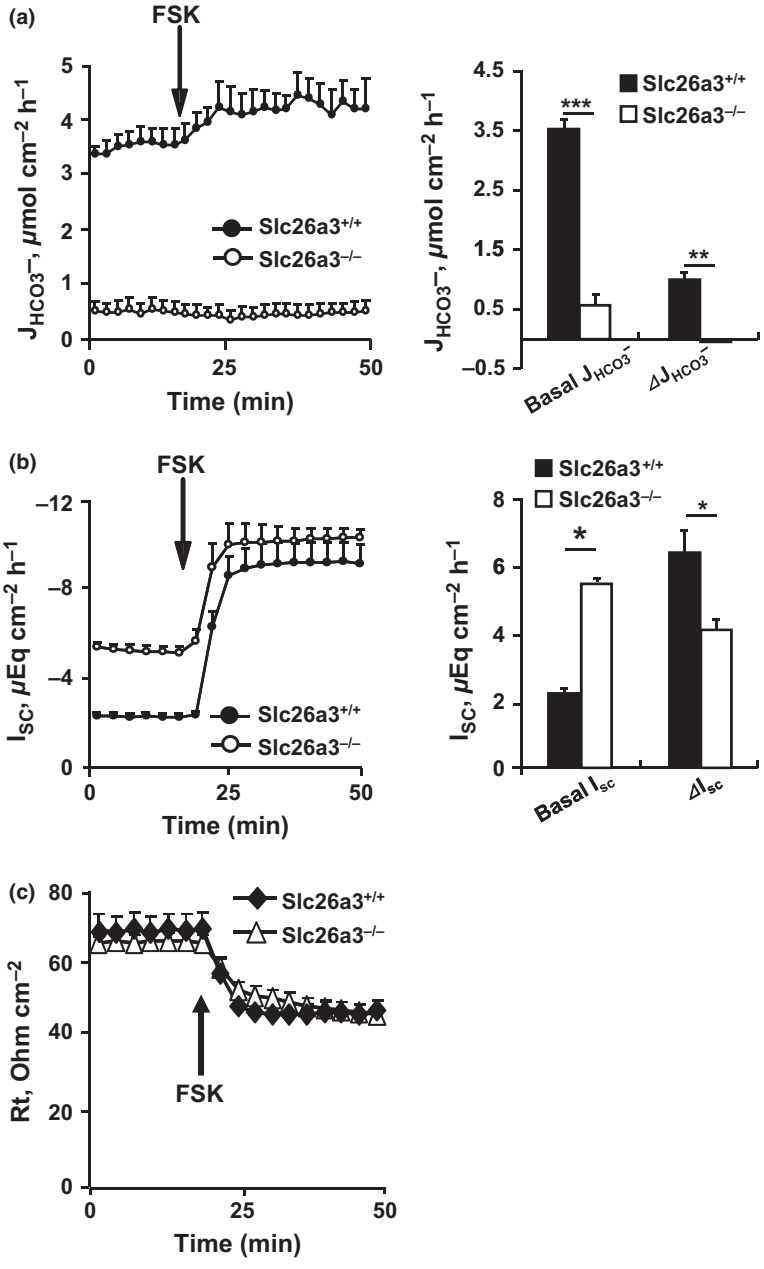


**Figure 1** $HCO_3^-$ secretory rates ($J_{HCO3}^-$) are strongly decreased and not responsive to FSK in Slc26a3$^{-/-}$ mid-distal colonic mucosa in vitro. (a) Time course (left panel) and bar graph (right panel) of luminal alkalinization ($J_{HCO3}^-$) in the basal state and after the serosal application of $10^{-5}$M FSK to isolated and Slc26a3$^{+/+}$ mid-distal colonic mucosa. (b) Calculated $I_{sc}$ (from tissue resistance $R_t$ and potential difference PD in open circuit) in Slc26a3$^{-/-}$ and Slc26a3$^{+/+}$ mid-distal colon. (c) Tissue resistance ($R_t$) was not significantly different in Slc26a3$^{-/-}$ and Slc26a3$^{+/+}$ mid-distal colonic mucosa and decreased to the same degree after FSK stimulation. *$P < 0.05$, **$P < 0.01$ and ***$P < 0.001$ vs. Slc26a3$^{+/+}$. $n = 5$.

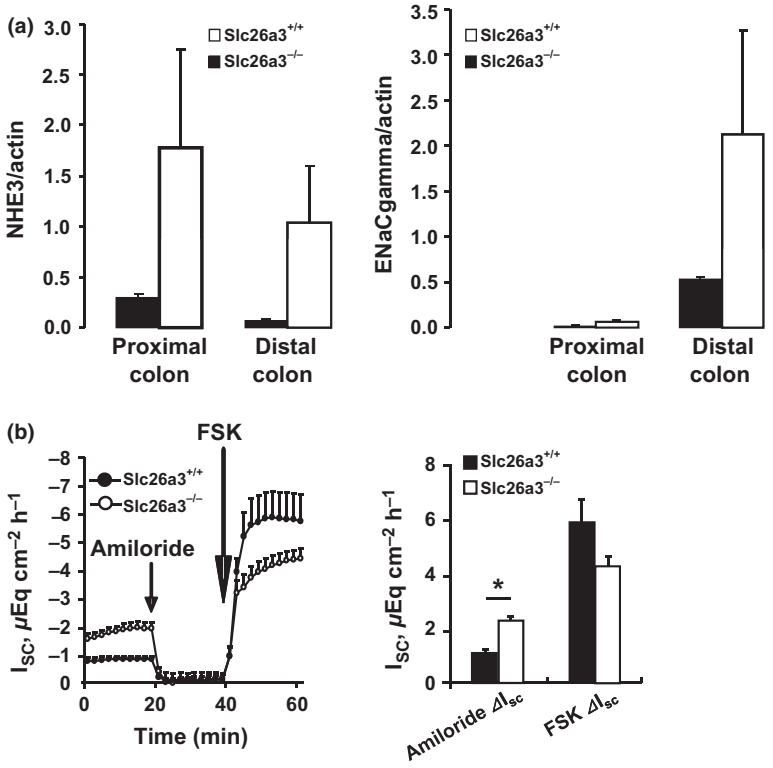


**Figure 2** NHE3 and ENaC mRNA expression and amiloride-sensitive $I_{sc}$ are increased in Slc26a3$^{-/-}$ mid-distal colon. (a) mRNA expression levels for NHE3 (left panel) and the ENaC $\gamma$-subunit (right panel) show upregulation of both genes in the Slc26a3$^{-/-}$ colon, although this did not reach statistical significance because of high variability in the knock-outs. (b) Short-circuit current response ($\Delta I_{sc}$) upon luminal amiloride ($10^{-5}$M) application (first arrow) in mid-distal colonic mucosa (short-circuited tissue, bilateral $CO_2/HCO_3^-$ buffers). At the second arrow, forskolin (FSK, $10^{-5}$M) was added to the serosal bath. *$P < 0.05$, vs. Slc26a3$^{+/+}$. $n = 4$–6.

sensitive and therefore likely to be mediated by an increase in ENaC activity, the expression of which was increased in the mid-distal colon of Slc26a3$^{-/-}$ mice (Fig. 2a, b). FSK elicited a strong $I_{sc}$ response in Slc26a3$^{-/-}$ and Slc26a3$^{+/+}$ mid-distal colonic mucosa (Figs 1b, 2b), but a $\Delta J_{HCO3^-}$ only in Slc26a3$^{+/+}$ mucosa (Fig. 1a), suggesting that CFTR activation is preserved (albeit possibly to a somewhat reduced extent) in Slc26a3$^{-/-}$ colon, but it does not seem to contribute to the secretion of $HCO_3^-$ in this experimental setting (Fig. 1a, b).

### *Reduced $HCO_3^-$ secretion and fluid absorption in the mid-distal colon of Slc26a3$^{-/-}$ mice* in vivo

Slc26a3$^{-/-}$ and Slc26a3$^{+/+}$ mouse mid-distal colon was luminally perfused in anaesthetized mice, and $J_{HCO3^-}$ and fluid absorptive rates were measured. The absence of DRA expression resulted in a very strong reduction in basal $J_{HCO3^-}$ compared to WT *in vivo* (Fig. 3a, b). Likewise, the secretory response to luminal perfusion with FSK was almost abolished (Fig. 3a, b), confirming the *in vitro* findings.

We also measured fluid absorption in Slc26a3$^{+/+}$ and Slc26a3$^{-/-}$ mid-distal colon and found that the colon of Slc26a3$^{-/-}$ mice was not in an absorptive mode, in contrast to the WT colon (Fig. 3c). This was surprising, because an increased expression of the $Na^+$ absorptive transporters had been described in the colon of Slc26a3$^{-/-}$ mice and was suggested to serve as a potential rescue mechanism against intestinal fluid loss (Schweinfest *et al.* 2006). Indeed, we also observed an increase in NHE3 and ENaC mRNA expression in the colon of our Slc26a3$^{-/-}$ mice (not significant because of a large SEM in Slc26a3$^{-/-}$ colon), despite the very intense nutritional treatment in this cohort (Fig. 2a). We therefore wondered about the membrane localization and functional activity of NHE3 in Slc26a3$^{-/-}$ mice and WT counterparts.

### *NHE3 mRNA and protein expression and acid-activated NHE3 activity in the colon of Slc26a3$^{-/-}$ mice*

NHE3 staining in the Slc26a3$^{-/-}$ surface colonocyte apical membranes both displayed more intense staining (Fig. 4a, WT, and Fig. 4b, Slc26a3$^{-/-}$) and the staining reached deeper into the cryptal mouths (Fig. 4a, b, lower magnification in the micrographs to the right side), compared to the same colonic segment in WT mice. When the localization of NHE3 in relationship to the F-actin staining of the microvillar membrane was studied (Fig. 4a, b, uppermost right curves), the peak of NHE3 pixel intensity was slightly more extracellular than the peak for F-actin. Because the F-actin is most intense in the terminal web region, this shift to the right of the peak of NHE3 pixel intensity compared to F-actin pixel intensity signifies that the NHE3 is located predominantly in the microvilli both in Slc26a3$^{+/+}$ and in Slc26a3$^{-/-}$ mid-distal colonic mucosa (Lin *et al.* 2010). Acid-activated NHE3 activity in the colonocytes

 

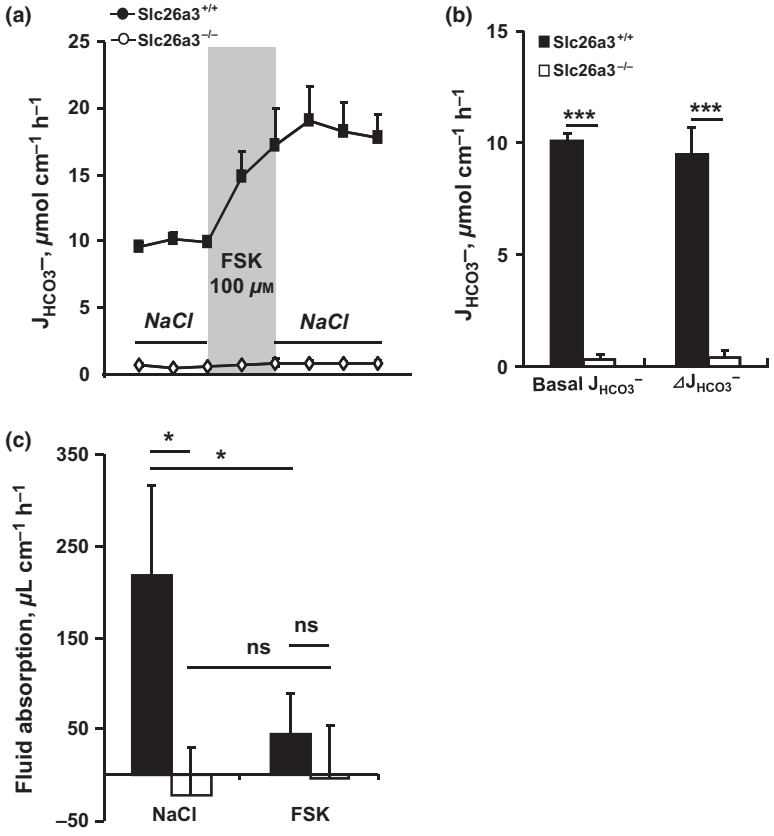


**Figure 3** Strong reduction of $J_{HCO3}^-$, no $\Delta J_{HCO3}^-$ response to FSK and loss of absorptive rate in the mid-distal colon of anaesthetized Slc26a3$^{-/-}$ mice. (a) Time course of $J_{HCO3}^-$ in a basal state and after luminal application of $10^{-4}$M FSK in the mid-distal colon of anaesthetized Slc26a3$^{-/-}$ and Slc26a3$^{+/+}$ mice. (b) $J_{HCO3}^-$ and FSK-induced $\Delta J_{HCO3}^-$. (c) Fluid absorptive/secretory rate in Slc26a3$^{-/-}$ and Slc26a3$^{+/+}$ mid-distal colon before and after FSK. *$P < 0.05$ and ***$P < 0.001$ vs. Slc26a3$^{+/+}$, $n = 5$.

of the cryptal mouth openings (where NHE3 is strongly expressed, Cinar *et al.* 2007) was significantly higher in Slc26a3$^{-/-}$ than in WT mice, when acidified to a similar degree ($pH_i$ 6.4–6.5) (Fig. 4c). A representative $pH_i$ trace of a single experiment is shown in the supplementary files (Figure S2).

Luminal application of the specific NHE3 inhibitor S1611 is known to cause a rise in luminal alkaline output in murine WT, but not NHE3-knockout duodenum, likely to be mediated by the inhibition of NHE3-mediated proton extrusion (Furukawa *et al.* 2005, Singh *et al.* 2010). This technique was therefore used to probe the basal (non-acid-activated) NHE3 activity in the murine colon *in vivo*. S1611 application elicited a significant rise in mid-distal colonic $HCO_3^-$ output in Slc26a3$^{+/+}$ mice, which was absent in Slc26a3$^{-/-}$ mice (Fig. 4d). This indicates that NHE3 is not actively exporting protons (and therefore not absorbing $Na^+$) in the Slc26a3$^{-/-}$ colonic mucosa in anaesthetized mice, despite its high expression level and its localization in the microvillar membrane.

### *Alkaline $pH_i$ may prevent NHE3-mediated fluid absorption*

We speculated that a reason for the lack of fluid absorption in the Slc26a3$^{-/-}$ colon may be a high $pH_i$ in the surface colonocytes, due to their inability to extrude $HCO_3^-$ into the lumen, which has been previously reported for Slc26a3$^{-/-}$ duodenal villus enterocytes (Walker *et al.* 2009). We therefore assessed the steady-state $pH_i$ in the Slc26a3$^{+/+}$ and Slc26a3$^{-/-}$ colonocytes. The steady-state $pH_i$ was significantly higher in Slc26a3$^{-/-}$ than in Slc26a3$^{+/+}$ colonocytes in the presence of $CO_2/HCO_3^-$, which is the likely physiological situation (Fig. 5a, b). At this high $pH_i$, NHE3 is expected to have very little activity (Orlowski 1993).

### *Slc26a3$^{-/-}$ colon lacks a normal inner mucus layer*

The colon was fixed in Carnoy, a method that preserves the mucus layer as shown before (Johansson *et al.* 2008). Immunohistochemical staining of these sections with an antiserum against the MUC2 mucin and visualization of the nuclei with DAPI revealed an adherent inner mucus layer that typically showed a stratified MUC2 and with a thickness of about 50 μm in the WT mice (Fig. 6A, left panel). No stratified, adherent inner Muc2-stained mucus layer was observed in the Slc26a3$^{-/-}$ colon (Fig. 6A, right panel). When a series of mice were studied, and the sections were taken at the same distance from the anal canal (approx. 3 cm), an adherent mucus layer was regularly observed in 5 of 5 WT mice (Fig. 6B, upper panels), but only in

 

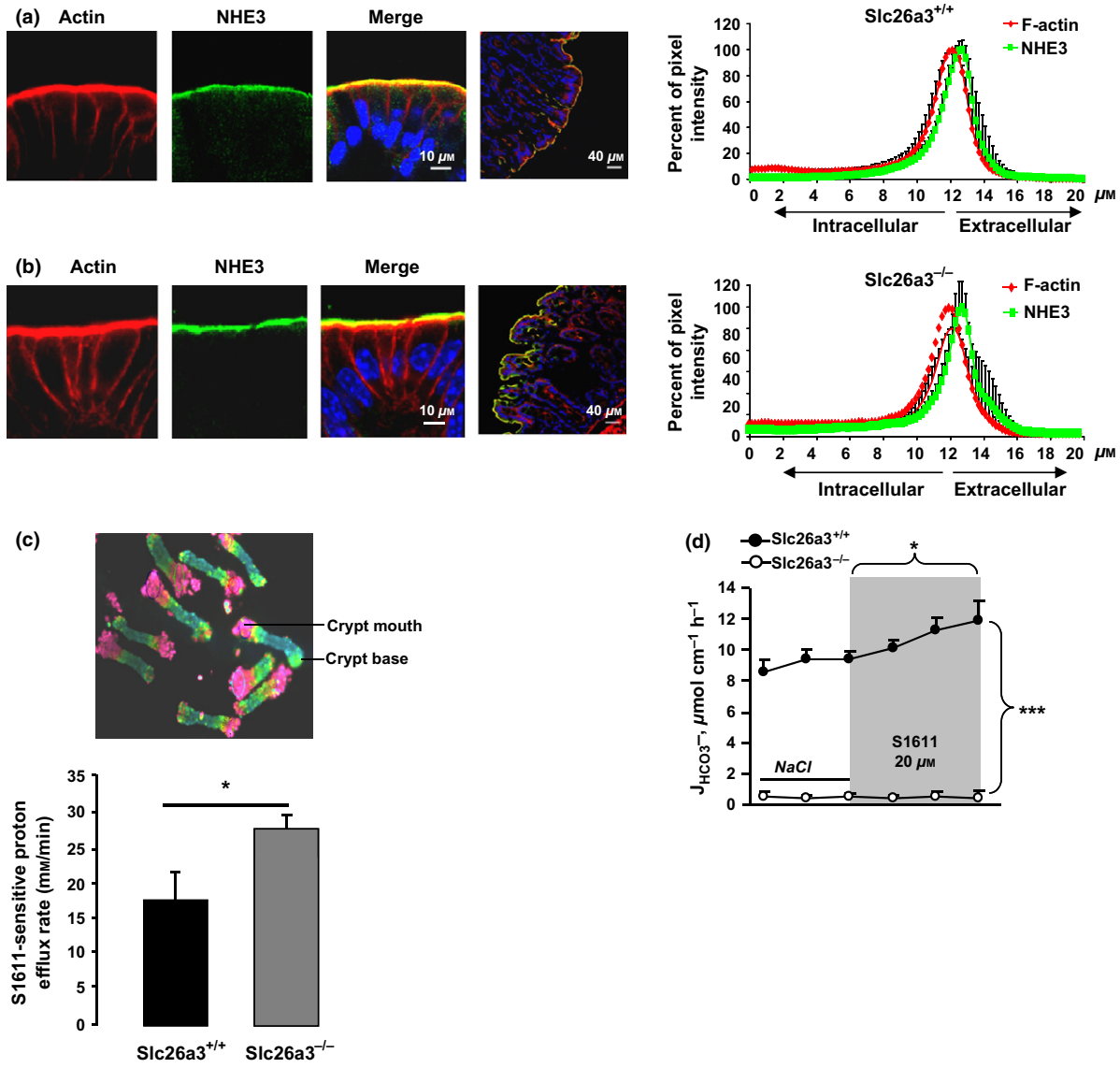


**Figure 4** Increased colonic brush border membrane abundance and acid-activated activity of NHE3 in Slc26a3$^{-/-}$ colonic crypts, but no evidence for NHE3-mediated $Na^+/H^+$ exchange in Slc26a3$^{-/-}$ colon in vivo. (a) Immunohistochemical staining of NHE3 (green) and F-actin (red) in the mid-distal colonic BBM membrane of WT and (b) Slc26a3$^{-/-}$ mice (a, b, left panels). Distribution of F-actin (red) and NHE3 (green curve) along the terminal web–microvillar axis was measured as described in Lin *et al.* (2010) with modifications described in Chen et al., (2010a) perpendicular to the microvillar axis. The peak of the F-actin indicates the terminal web/microvillar cleft region. Both in Slc26a3$^{-/-}$ and in WT mice, NHE3 was found predominantly in the membrane. Scale bar sizes indicated in the graphs. (c) Acid-activated NHE3 activity was measured fluorometrically in the cryptal mouth of isolated mid-distal colonic crypts of WT and DRA KO mice [the region of red pseudocolour staining in the image of BCECF-loaded WT crypts, which are the cells that display rapid $pH_i$ recovery in the presence of Hoe 642] and found to be significantly increased in the Slc26a3$^{-/-}$ colonic crypts. Specificity for NHE3 was obtained by performing two consecutive ammonium prepulses and adding 20 $\mu$M specific NHE3 inhibitor S1611 to the second pulse (a $pH_i$ trace showing the experimental design can be found in Figure S2). Proton flux rate, calculated from the initial $pH_i$ recovery/time x intrinsic buffer capacity at the given $pH_i$, after the second pulse, was subtracted from that after the first pulse $^*P < 0.05$, $n = 6$–8. (d) Time course of $J_{HCO3}^-$ in a basal state and after luminal application of 20 $\mu$M S1611 in the mid-distal colon of anaesthetized Slc26a3$^{-/-}$ and Slc26a3$^{+/+}$ mice. An increase in alkalinization rate $J_{HCO3}^-$ was only seen in the WT mice. $^*P < 0.05$ and $^{***}P < 0.001$ vs. Slc26a3$^{+/+}$, $n = 5$.

1 of 5 DRA KO mice was any layer observed at all, which appeared thinner and less well stratified, and the other images showed no layer (Fig. 6B, lower panels). However, no increased bacteria count at the epithelial surfaces of the DRA KO mid-distal colon, such as seen for the MUC2 KO (Johansson *et al.* 2008, Fu *et al.*

 

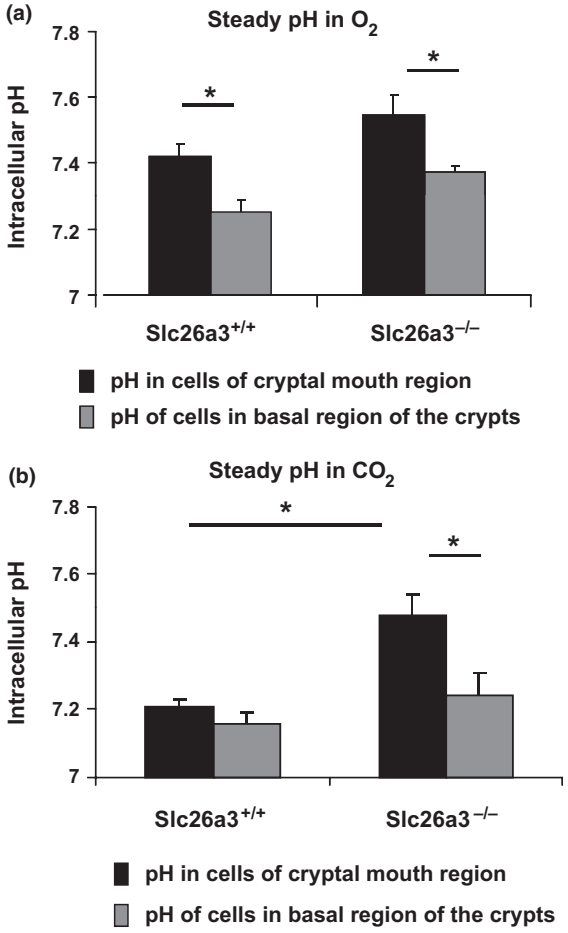


**Figure 5** Steady-state $pH_i$ in the cryptal mouth and the cryptal base regions of Slc26a3$^{-/-}$ and WT colonic crypts. (a) In the absence of exogenous $CO_2/HCO_3^-$, steady-state $pH_i$ was higher in the Slc26a3$^{-/-}$ than in WT colonic crypts, but this did not reach the level of significance. In addition, the $pH_i$ was significantly higher in the cryptal mouth than in the base region, both in WT and in Slc26a3$^{-/-}$crypts. (b) In the presence of $CO_2/HCO_3^-$, $pH_i$ was significantly lower in the cryptal mouth region of WT compared to Slc26a3$^{-/-}$ crypts, as well as significantly lower in the presence $CO_2/HCO_3^-$ than in the absence of $CO_2/HCO_3^-$ in the surface but not the crypt colonocytes. This indicates that Slc26a3 function lowers $pH_i$ in the colonic cells where it is expressed [the surface/cryptal mouth region of the colonic epithelium (Jacob *et al.* 2002, Lamprecht *et al.* 2002, Xiao *et al.* 2012a). *$P < 0.05$, $n = 5$–6]

2011) or in patients with Crohn's disease (Kleessen *et al.* 2002, Swidsinski *et al.* 2005), or, interestingly, in NHE3 KO mice which do have a firm mucus layer (Figure S3), was noted.

The number of goblet cells was counted in mid-distal colonic mucosa of Slc26a3$^{-/-}$ and Slc26a3$^{+/+}$ mice in serial sections at a similar distance from the anus and was not found significantly altered in Slc26a3$^{-/-}$ vs. WT mid-distal colon (Fig. 6C).

### *Slc26a3$^{-/-}$ colon is highly susceptible to DSS damage*

The observed lack of inner mucus layer in the mid-distal colon (Fig. 6A-C) suggests that the protective properties of the mucus may be altered (Johansson *et al.* 2008, Fu *et al.* 2011). To test the susceptibility of Slc26a3$^{-/-}$ to colonic injury, we used the DSS model of colitis induction, because this model has been previously studied to assess the time sequence of mucus layer collapse, bacterial penetration and onset of inflammation (Johansson *et al.* 2010a,b). We first established an acute DSS colitis standard protocol, using 2, 4 or 6% DSS in the drinking water for 7 days to see the colitis severity after different concentrations of DSS treatment (Figure S1). Slc26a3$^{-/-}$ mice proved extremely susceptible to the development of severe disease shortly after the application to even low concentrations of DSS (2%) to the drinking water, while the WT littermates showed only slight inflammation in the colon at the same exposure time ($n = 5$). At day 5 of DSS exposure, all Slc26a3$^{-/-}$ mice had died or been killed because of severe disease, while all Slc26a3$^{+/+}$ mice survived (Fig. 7A). The colons were fixed and their histology was compared. The colon of Slc26a3$^{-/-}$ mice treated for as little as 2 days with DSS already showed ulcerations and damaged epithelia (Fig. 7Ba) and signs of erythrocyte extravasation (Fig. 7Bd) into the lumen. These mice also showed larger and more frequent mucosal and submucosal lymphocyte accumulations than the WT mice (Fig. 7Bc, D). These histological pictures were different from the typical appearance of colitis after 7 days with 4–6% DSS, where a widespread damage to the mucosa was observed (Figure S1). In addition, even at large magnification, the epithelial surface of the Slc26a3$^{-/-}$ colon completely lacked any adherent mucus, which could still be observed (although not continuous) after the DSS exposure in WT mice (Figure S4).

## Discussion

The mid-distal colon is an intestinal segment with very high DRA expression level, and this corresponded to very high luminal alkalinization level both in isolated epithelium *in vitro* and in the anaesthetized mouse *in vivo*, which were very strongly reduced in Slc26a3$^{-/-}$ mid-distal colon. In addition, this segment of Slc26a3$^{-/-}$ intestine was not able to absorb fluid *in vivo*, in contrast to the more proximal intestinal segments, which are able to absorb fluid in the absence and more so in the presence of luminal nutrients (Xia *et al.* 2013). This fluid absorptive defect in the mid-distal colon correlated with some clear liquid being passed via the anus together with pasty stool.

 

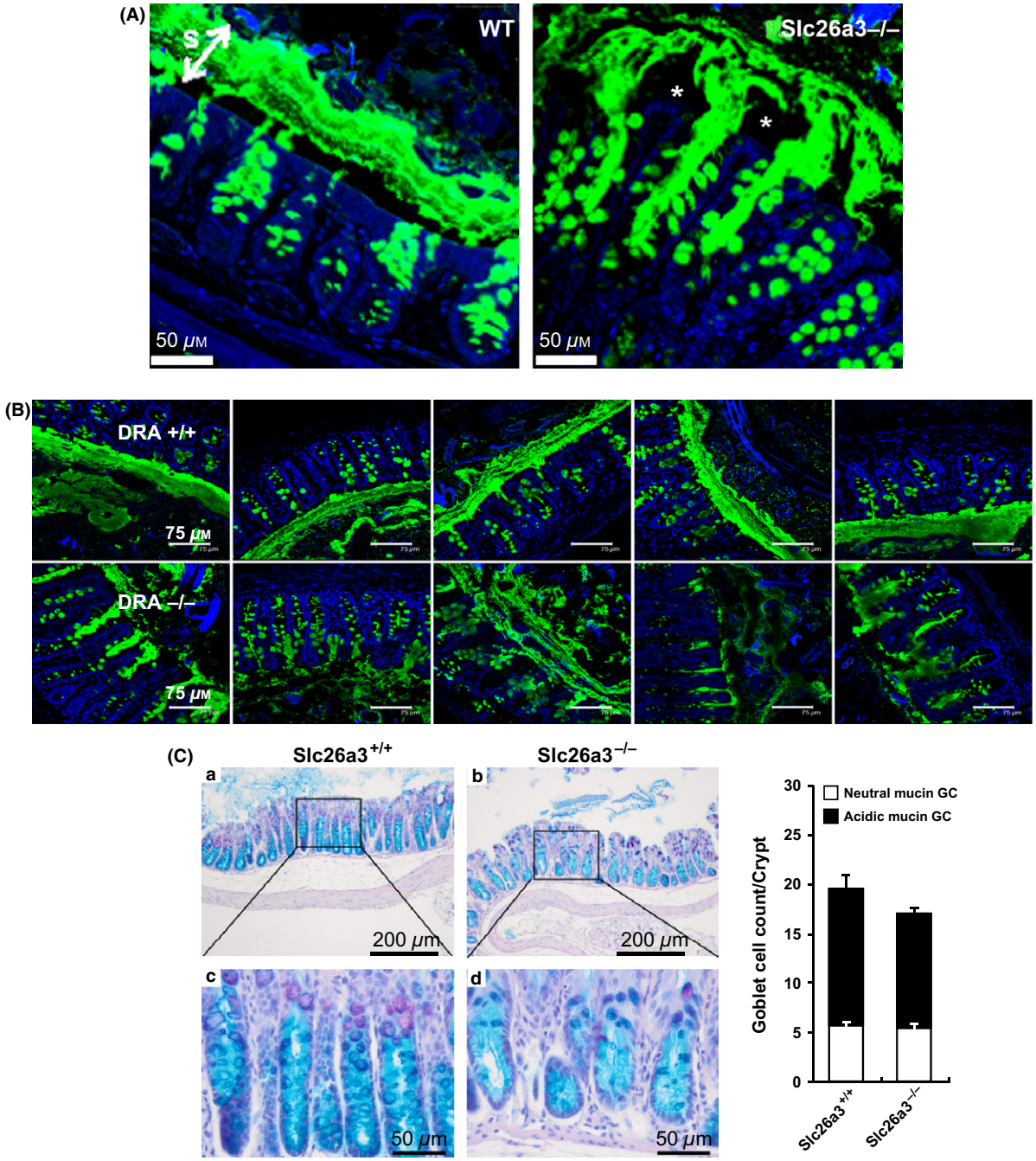


**Figure 6** Similar goblet cell number but altered inner mucus layer in Slc26a3$^{-/-}$ colon. (A) Carnoy-fixed colon tissue immunostained with an antiserum against MUC2 mucin (anti-MUC2C3, green fluorescence). Blue DAPI stains the nuclei of the colonic epithelial cells. The WT mice show a well-stratified normal inner mucus layer (labelled s) that is about 50 $\mu$m thick. In the Slc26a3$^{-/-}$ mice, there is no normal mucus layer, and instead, MUC2 is shown to form large mucus plumes filled with empty liquid-filled cavities (marked *). Scale bar is 50 $\mu$m. (B) A panel of lower magnification MUC2 stainings in additional mice is shown in Figure 6B. While 5 of 5 WT mid-distal colons displayed a stratified adherent mucus layer (upper panels), only 1 of 5 Slc26a3$^{-/-}$ mid-distal colons displayed any kind of layer formation, and this was discontinuous and thinner than in WT colon. $n$ = 5. (C) Alcian blue/PAS stain of Slc26a3$^{+/+}$ and Slc26a3$^{-/-}$ mid-distal colonic mucosa and the distribution of acidic mucin (bright blue) and neutral mucin (dark blue/violet) containing goblet cells along the crypt column of Slc26a3$^{+/+}$ and Slc26a3$^{-/-}$ mid-distal colon. Slides from seven mice were analysed and the tissue taken from the same distance from the anus. No significant difference in either type of goblet cell per crypt was detected. Scale bar sizes indicated in the graphs.

 

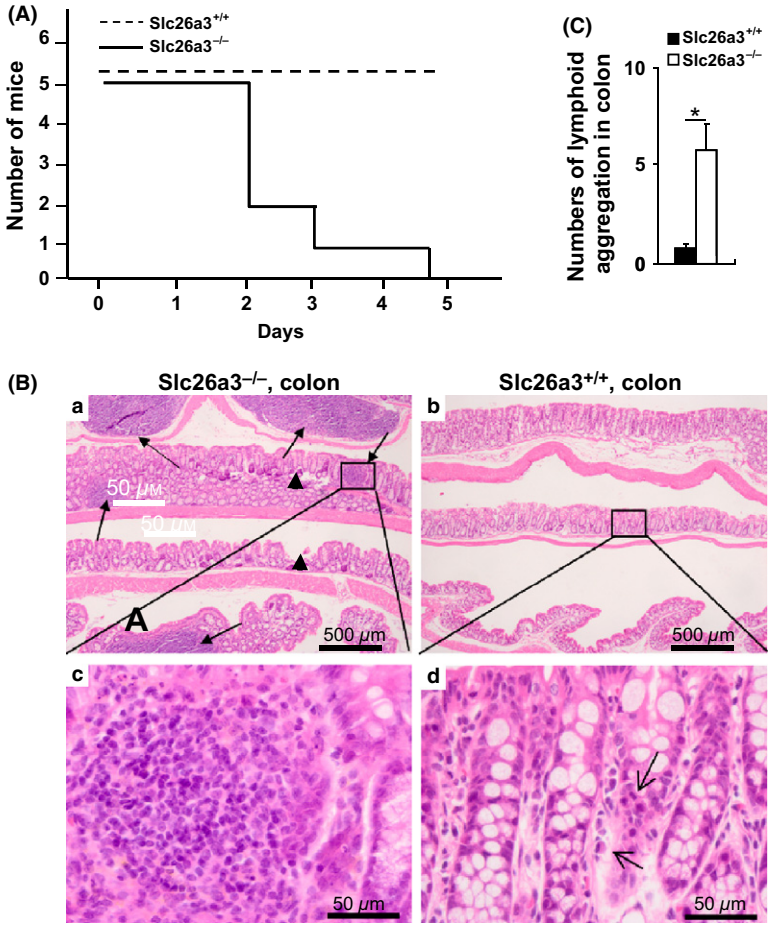


**Figure 7** Increased susceptibility of Slc26a3$^{-/-}$ mice to DSS damage. (A) Survival curves of the Slc26a3$^{-/-}$ and Slc26a3$^{+/+}$ mice ($n$ = 5) given 2% DSS in their drinking water. The Slc26a3$^{-/-}$ died or had to be killed due to severe bleeding, whereas all Slc26a3$^{+/+}$ survived all 5 days. (B) Formaldehyde-fixed Swiss rolls of colon stained with H&E. The Slc26a3$^{-/-}$ mice (Figure 7B a,c) treated with 2% DSS for only 2–3 days show numerous ulcerations (arrowhead) and damages to the epithelial cells layer in comparison with WT (Figure 7B b,d). An increase in the size and number of lymphoid aggregates (closed arrow) was also observed in the Slc26a3$^{-/-}$ mouse colon after 2% DSS, whereas only slight neutrophils infiltrated into mucosa (open arrow) after 2–3 days of 2% DSS treatment in WT colon. Scale bar sizes indicated in the graphs. (C) Lymphoid aggregates were counted in the entire fixed Swiss role of colon, and the number was significantly higher in the Slc26a3$^{-/-}$ than in the Slc26a3$^{+/+}$ colon. $P < 0.05$, $n = 5$.

The complete lack of fluid absorption in the mid-distal colon was unexpected, because a previous report had proposed that the observed very strong upregulation of NHE3 and ENaC expression in this part of the intestine may serve as a rescue mechanism to ensure fluid and electrolyte uptake (Schweinfest *et al.* 2006). Indeed, we had observed a reduction by only approx. 30% of fluid absorptive rate during saline perfusion in Slc26a3$^{-/-}$ jejunum, where no upregulation of NHE3 mRNA or protein was observed (Xia *et al.* 2013). We also observed an increase in ENaC-mediated $I_{sc}$ in the distal colonic mucosa *in vitro* of Slc26a3$^{-/-}$ compared to WT mice (Fig. 2b) and a significant increase in acid-activated NHE3 transport in crypts isolated from that region of the colon (Fig. 4c). Despite ENaC and NHE3 upregulation, the mid-distal colon was not in the fluid absorptive state and did not show evidence of NHE3-mediated transport *in vivo*. We assume that the high steady-state $pH_i$ of Slc26a3$^{-/-}$ colonic enterocytes (Fig. 5) is responsible for the low NHE3 activity in Slc26a3$^{-/-}$ colon, because the pH dependence of NHE3 would predict low or absent NHE3 transport at this high $pH_i$ (Orlowski 1993) and because NHE3 activity could be stimulated in Slc26a3$^{-/-}$ colonic enterocytes to even higher proton extrusion rates than in WT enterocytes after an ammonium prepulse (which will acidify the cells) (Fig. 4c). The reason for the lack of absorption in the Slc26a3$^{-/-}$ distal colon may therefore be both the absence of the major transcellular $Cl^-$ uptake pathway and a silent NHE3 because of the high $pH_i$ of Slc26a3$^{-/-}$ colonocytes. Why we do not see ENaC-mediated absorption in the distal colon of Slc26a3$^{-/-}$ mice is unclear at present.

Blood gas analysis from blood drawn prior to correction by infusion of electrolyte solution in the Slc26a3$^{-/-}$ and Slc26a3$^{+/+}$ mice are consistent with the expected alterations in CLD patients, but differed significantly from those described previously in Slc26a3$^{-/-}$ mice (Walker *et al.* 2008). We did not observe the low blood pH described in both Slc26a3$^{-/-}$ and more so in Slc26a3$^{+/+}$ mice in that study, which may in part be due to a different anaesthesia protocol or a different feeding schedule. To obtain Slc26a3$^{-/-}$ mice with sufficient age and body weight for *in vivo* experiments, we not only provided them with the drinking solutions as suggested by Walker *et al.* (2008) but we also fed them a low-fat, energy-rich diet, which

had to be made into a paste. This resulted in significantly prolonged survival and better weight/growth parameters, and may have had impact on energy and fluid balance, as well as blood gas parameters. We still observed a (non-significant) upregulation of distal colonic ENaC $\gamma$-unit, a sensitive marker for hyperaldosteronism that appeared mild compared to a previous report (Schweinfest *et al.* 2006) (Fig. 2b).

In addition to the very low basal $HCO_3^-$ output, the Slc26a3$^{-/-}$ colon displayed no $HCO_3^-$ secretory response to FSK. CFTR $Cl^-$ conductance was activated by FSK in Slc26a3$^{-/-}$ colon, as evidenced by a robust $I_{sc}$ response (Figs 1b, 2b), but this did not result in $HCO_3^-$ secretion. One likely reason for this is that a part of FSK-induced increase in luminal alkalinization was previously found to be via cAMP-mediated inhibition of NHE3 (Xiao *et al.* 2012b), and NHE3 activity was low in Slc26a3$^{-/-}$ colon. Another contributing factor to the lack of FSK-induced $HCO_3^-$ secretory response may be that CFTR and Slc26a3 expression overlap in the mid-region of the crypt–surface axis, and in this case, Slc26a3 may serve as a $Cl^-$ recycling pathway during CFTR-mediated $Cl^-$ secretion, resulting in CFTR-activation dependent, Slc26a3-mediated $HCO_3^-$ output. This part of FSK-stimulated $HCO_3^-$ output would be lost in the absence of Slc26a3 expression (Xiao *et al.* 2012b).

An inability to secrete $HCO_3^-$ has been linked to disturbed mucus expansion and mucus hydration in the intestine and other epithelia (Garcia *et al.* 2009, Chen *et al.* 2010b, Yang *et al.* 2013), corresponding to a more pronounced adherent mucus layer in the colon of CF mice (Parmley & Gendler 1998, Musch *et al.* 2013). To visualize the colon mucus, we performed MUC2 immunohistochemistry on mid-distal colonic tissues fixed in Carnoy, a method known to preserve the mucus (Johansson *et al.* 2008). The inner mucus layer in the colon of WT mice appeared well organized with a clear stratified appearance, due to the net-like structure of the MUC2 mucin polymer (Johansson *et al.* 2010a,b). In the Slc26a3$^{-/-}$ mice, this mucus organization was absent. It is thus clear that the colonic firmly adherent mucus is not normal in the Slc26a3$^{-/-}$ mice and that this is likely to have an impact on the properties of the inner mucus layer.

It is unclear at this time why Slc26a3$^{-/-}$ colon does not display a normal mucus layer, but one reason may be the very low $HCO_3^-$ output rates and the complete lack of fluid absorption. It has recently been shown that the MUC2 mucin is packed due to information in the N-terminal end of MUC2 in the goblet cell granules with a pH of 6 and high calcium (Ambort *et al.* 2012). Upon secretion, the mucin normally expands >1000-fold, something that may require a raised pH and removal of calcium, which, due to its low luminal alkalinization rate, the Slc26a3$^{-/-}$ colon may not accomplish. Further investigations are necessary to better understand the reasons for a lack of firm mucus layer in Slc26a3$^{-/-}$ mid-distal colon.

Mucus layer collapse has been associated with the onset of inflammation in a mouse model of DSS colitis (Johansson *et al.* 2010a,b), and the absence of a mucus layer in the MUCc2-deficient mice was also associated with spontaneous colitis development (Van der Sluis *et al.* 2006 , Johansson *et al.* 2008). In contrast to the MUC2-deficient colon, which displays bacteria penetrating into the crypt depth (Johansson *et al.* 2008), the Slc26a3$^{-/-}$ colon does not show bacteria in the crypts, although a detailed study was not performed. On the other hand, the Slc26a9$^{-/-}$ (NHE3-deficient) mid-distal colon shows an adherent mucus layer which is nevertheless full of bacteria (Figure S3). This mouse strain develops spontaneous colitis (Laubitz *et al.* 2008), and in contrast to the Slc26a3$^{-/-}$ distal colon, the distal colon of the Slc26a9$^{-/-}$ mouse is hyper-resorptive, at least in our hands, due to upregulation of other $Na^+$ absorptive pathways that partially compensate the defect in fluid absorption in the small intestine (Xia *et al.* 2013, J.Li, unpublished observations), and overcompensate in the Slc9a3$^{-/-}$ colon (compared to the same segment in the WT mice). On the other hand, the Slc26a9$^{-/-}$ colon has a secretory defect, similar to the CFTR$^{-/-}$ colon (Xiao *et al.* 2012b), which may result in mucus stasis and loss of the flushing response of the crypts.

In order to evaluate the pathophysiological significance of a structurally altered adherent mucus layer in the absence of obvious bacterial adherence to the mucosa, we assessed the susceptibility of the Slc26a3$^{-/-}$ mouse to DSS damage. Slc26a3 deficiency resulted in a remarkable decrease in mucosal resistance against DSS-induced colitis. We were surprised to see that even 2% DSS in the drinking water had very severe effects on intestinal health. In the cohort, all five WT mice had no symptoms and minor histological sign of inflammation at 2–3 days after the start of DSS drinking, while the Slc26a3$^{-/-}$ mice had already either died or had to be killed. The Slc26a3$^{-/-}$ mice developed severe bloody diarrhoea and ulcerations in the epithelium. Histologically, an increase in size and number of the lymphoid aggregates in the mucosa was seen in Slc26a3$^{-/-}$ DSS-treated mice, which could also be found in WT mice but not in this size and frequency. This increase in size and frequency of lymphoid aggregates in the colon has also been observed in other mouse models with a defect in mucosal barrier or immune function during the development of intestinal inflammation (Laukoetter *et al.* 2007, Lochner *et al.* 2011), and it has also been described for the

 

MUC2-deficient mice (Van der Sluis *et al.* 2006, Petersson *et al.* 2011). DSS has a cell-toxic effect and causes the mucus layer to become permeable to bacteria (Johansson *et al.* 2010a,b, Petersson *et al.* 2011). We assume that the lack of an inner mucus layer is a primary reason for the strongly increased susceptibility of the Slc26a3$^{-/-}$ mice to DSS damage. However, other possibilities have to be taken into account. Could an impairment in the paracellular pathway be a reason for the increased susceptibility of the Slc26a3$^{-/-}$ mice to DSS colitis? The electrical resistance was not different in Slc26a3$^{-/-}$ compared to Slc26a3$^{+/+}$ colonic mucosa (Fig. 1), and the $HCO_3^-$ flux into the luminal bath was exceedingly low, despite a high concentration gradient for $HCO_3^-$ into the lumen. We have previously observed that the mildly inflamed proximal colon of TNF$^{\Delta are}$ heterozygote mice displays slightly increased mannitol flux, a slight loss of cation selectivity and – the most significant difference in comparison with non-inflamed WT – an increased $HCO_3^-$ leak into the luminal solution (Juric *et al.* 2013). The extremely low $HCO_3^-$ efflux in the Slc26a3$^{-/-}$ colonic mucosa *in vivo* and *in vitro* suggests to us that a leaky barrier is an unlikely reason for the increased susceptibility to DSS. Another reason for not pursuing the question of a potential alteration of the tight junctional pathway in Slc26a3$^{-/-}$ colon further is that the claudins that constitute the tight junctional complexes in the surface area of the native murine mid-distal colon are functionally not well characterized, and thus, no clear-cut study targets exist for this question (Fujita *et al.* 2006, Holmes *et al.* 2006).

We believe that the most likely explanation for the enormously increased susceptibility to DSS damage is the defective extracellular milieu, including the loss of luminal alkalinization and the lack of a firm mucus layer. Early experiments on gastric, duodenal as well as colonic epithelium demonstrated a rapid repair of superficially injured areas by a process called 'rapid epithelial restitution' (Lacy 1988, Riegler *et al.* 1991). An acidic luminal pH delayed this process in the epithelia where this issue was tested. Thus, it is feasible, even likely, that the process of epithelial restitution is continuing during DSS colitis induction and that it may be negatively affected by the low luminal pH in the Slc26a3$^{-/-}$ colon. In contrast, the high intracellular $pH_i$ of DRA enterocytes, which has also been measured in the duodenum (Walker *et al.* 2009), may be one reason that explains why, despite an abnormal acid-induced $HCO_3^-$ secretory rate (Singh *et al.* 2013), neither CLD patients nor Slc26a3$^{-/-}$ mice have been reported to show an increased incidence of duodenal ulcerations. A similar situation has been described in CF patients and CFTR-deficient or CFTR-inhibited rodents and called the 'CF paradox' (Kaunitz & Akiba 2001). However, the high $pH_i$ did not protect against DSS colitis. Further work is required to delineate the epithelial abnormalities in wound repair in the Slc26a3$^{-/-}$ colon. Based on the similarity of the basic defect, we strongly believe that a similar defect in the mucus layer also exists in the colon of CLD patients and that this contributes to the increased incidence of acute and chronic intestinal inflammation in this patient population. However, the colonic mucus layer has, to our knowledge, not been studied in CLD patients.

The findings of this study are also interesting in view of the recent observation of a strong decrease in DRA expression and luminal $HCO_3^-$ output in inflamed colon (Xiao *et al.* 2012a). Based on the results of the present study, it is tempting to speculate that the low $HCO_3^-$ output observed in intestinal inflammatory disorders may well be a factor in maintaining chronic inflammation, adding to the vicious cycle of inflammation weakening the intestinal barrier properties and *vice versa*.

In summary, the loss of DRA expression virtually abolishes murine mid-distal colonic alkalinization rates. This intestinal segment displays no active fluid absorption in the Slc26a3$^{-/-}$ mouse despite a strong upregulation in the expression of sodium absorptive transporters, probably because the abnormally high surface colonocyte $pH_i$ prevents their activation *in vivo*. The generation of an adherent inner mucus layer is disturbed in Slc26a3$^{-/-}$ colon. Concomitantly, the mid-distal colonic mucosa displays a strikingly increased susceptibility to DSS injury. Nevertheless, the Slc26a3$^{-/-}$ distal colon of our mice did not display features of crypt elongation and mucosal ulcerations seen in other colitis mouse models such as the Muc2-deficient or IL-10-deficient mice. The results are consistent with an only mildly increased incidence of inflammatory bowel disease in CLD patients (Hihnala *et al.* 2006) and a mild but significant impact of a single-nucleotide polymorphism in the *Slc26a3* gene with ulcerative colitis incidence in the Japanese population (Asano *et al.* 2009). They provide evidence for a relationship between colonic electrolyte and acid/base transport, properties of the firmly adherent mucus layer and epithelial susceptibility to toxic injury and may help form a basis for understanding the increased incidence of intestinal inflammation in CLD patients.

## Conflict of interest

The authors have nothing to disclose.

We thank Brigitte Rausch, Natascha Cirpka, Silke Thiele and Denise Renner for their help with the animal breeding and genotyping. We thank Andrew Short for helpful advice with the style of the manuscript.

  doi: 10.1111/apha.12220

## Funding

This work was supported by the Deutsche Forschungsgemeinschaft Grants Nr. SFB621-C9 and Se460/13-4 (to U.S.), a HILF grant from Hannover Medical School (to A.K.S), a project grant from the Mukoviszidose e.V. Fördervereinigung (German mucoviszidosis foundation) to U.S., the Swedish Research Council (no. 7461, 21027), Torsten och Ragnar Söderbergs Stiftelser and The Swedish Foundation for Strategic Research – The Mucus-Bacteria-Colitis Center (MBC) of the Innate Immunity Program (2010–2014) (to G. H) and NSFC-81100264 (to F.X).

## Author's contribution

F.X., Q.Y., J.L., ME.V.J., A.K.S., W.X., B. R., R.E. and U.S. performed experiments and analysed results; M.M., M.S., D.T., G.X. and G.C.H. supplied experimental tools and gave extensive advice; F.X., A.K.S., G.C.H. and U.S. designed experiments and wrote the paper.

## References

Alper, S.L., Stewart, A.K., Vandorpe, D.H., Clark, J.S., Horack, R.Z., Simpson, J.E., Walker, N.M. & Clarke, L.L. 2011. Native and recombinant Slc26a3 (downregulated in adenoma, Dra) do not exhibit properties of $2Cl^-$/$1HCO_3^-$ exchange. *Am J Physiol* **300**, C276–C286.

Ambort, D., Johansson, M.E., Gustafsson, J.K., Nilsson, H.E., Ermund, A., Johansson, B.R., Koeck, P.J., Hebert, H. & Hansson, G.C. 2012. Calcium and pH-dependent packing and release of the gel-forming MUC2 mucin. *Proc Natl Acad Sci USA* **109**, 5645–5650.

Asano, K., Matsushita, T., Umeno, J., Hosono, N., Takahashi, A., Kawaguchi, T., Matsumoto, T., Matsui, T., Kakuta, Y., Kinouchi, Y. *et al.* 2009. A genome-wide association study identifies three new susceptibility loci for ulcerative colitis in the Japanese population. *Nat Genet* **41**, 1325–1329.

Bachmann, O., Riederer, B., Rossmann, H., Groos, S., Schultheis, P.J., Shull, G.E., Gregor, M., Manns, M.P. & Seidler, U. 2004. The $Na^+/H^+$ exchanger isoform 2 is the predominant NHE isoform in murine colonic crypts and its lack causes NHE3 upregulation. *Am J Physiol Gastrointest Liver Physiol* **287**, G125–G133.

Broere, N., Chen, M., Cinar, A., Singh, A.K., Hillesheim, J., Riederer, B., Lünnemann, M., Rottinghaus, I., Krabbenhöft, A., Engelhardt, R. *et al.* 2009. Defective jejunal and colonic salt absorption and altered $Na^+/H^+$ exchanger 3 (NHE3) activity in NHE regulatory factor 1 (NHERF1) adaptor protein-deficient mice. *Pflugers Arch* **457**, 1079–1091.

Chen, M., Sultan, A., Cinar, A., Yeruva, S., Riederer, B., Singh, A.K., Li, J., Bonhagen, J., Chen, G., Yun, C., Donowitz, M., Hogema, B., de Jonge, H. & Seidler, U. 2010a. Loss of PDZ adaptor protein NHERF2 affects membrane localization and cGMP- and [Ca2+]- but not cAMP-dependent regulation of Na+/H+ exchanger 3 in murine intestine. *J Physiol (Lond)* **588**, 5049–5063.

Chen, E.Y., Yang, N., Quinton, P.M. & Chin, W.C. 2010b. A new role for bicarbonate in mucus formation. *Am J Physiol Lung Cell Mol Physiol* **299**, L542–L549.

Cinar, A., Chen, M., Riederer, B., Bachmann, O., Wiemann, M., Manns, M., Kocher, O. & Seidler, U. 2007. NHE3 inhibition by cAMP and $Ca_2^+$ is abolished in PDZ-domain protein PDZK1-deficient murine enterocytes. *J Physiol* **581**, 1235–1246.

Fu, J., Wei, B., Wen, T., Johansson, M.E., Liu, X., Bradford, E., Thomsson, K.A., McGee, S., Mansour, L., Tong, M. *et al.* 2011. Loss of intestinal core 1-derived O-glycans causes spontaneous colitis in mice. *J Clin Invest* **121**, 1657–1666.

Fujita, H., Chiba, H., Yokozaki, H., Sakai, N., Sugimoto, K., Wada, T., Kojima, T., Yamashita, T. & Sawada, N. 2006. Differential expression and subcellular localization of claudin-7, -8, -12, -13, and -15 along the mouse intestine. *J Histochem Cytochem* **54**, 933–944.

Furukawa, O., Hirokawa, M., Zhang, L., Takeuchi, T., Bi, L.C., Guth, P.H., Engel, E., Akiba, Y. & Kaunitz, J.D. 2005. Mechanism of augmented duodenal $HCO_3^-$ secretion after elevation of luminal CO2. *Am J Physiol Gastrointest Liver Physiol* **288**, G557–G563.

Garcia, M.A., Yang, N. & Quinton, P.M. 2009. Normal mouse intestinal mucus release requires cystic fibrosis transmembrane regulator-dependent bicarbonate secretion. *J Clin Invest* **119**, 2613–2622.

Giulietti, A., Overbergh, L., Valckx, D., Decallonne, B., Bouillon, R. & Mathieu, C. 2001. An overview of real-time quantitative PCR: applications to quantify cytokine gene expression. *Methods* **25**, 386–401.

Hegyi, P., Rakonczay, Z. Jr, Gray, M.A. & Argent, B.E. 2004. Measurement of intracellular pH in pancreatic duct cells: a new method for calibrating the fluorescence data. *Pancreas* **28**, 427–434.

Hihnala, S., Höglund, P., Lammi, L., Kokkonen, J., Ormälä, T. & Holmberg, C. 2006. Long-term clinical outcome in patients with congenital chloride diarrhoea. *J Pediatr Gastroenterol Nutr* **42**, 369–375.

Holmes, J.L., Van Itallie, C.M., Rasmussen, J.E. & Anderson, J.M. 2006. Claudin profiling in the mouse during postnatal intestinal development and along the gastrointestinal tract reveals complex expression patterns. *Gene Expr Patterns* **6**, 581–588.

Jacob, P., Rossmann, H., Lamprecht, G., Kretz, A., Neff, C., Lin-Wu, E., Gregor, M., Groneberg, D.A., Kere, J. & Seidler, U. 2002. Down-regulated in adenoma mediates apical $Cl^-/HCO_3^-$ exchange in rabbit, rat, and human duodenum. *Gastroenterology* **122**, 709–724.

Johansson, M.E., Phillipson, M., Petersson, J., Velcich, A., Holm, L. & Hansson, G.C. 2008. The inner of the two Muc2 mucin-dependent mucus layers in colon is devoid of bacteria. *Proc Natl Acad Sci USA* **105**, 15064–15069.

Johansson, M.E., Gustafsson, J.K., Sjöberg, K.E., Petersson, J., Holm, L., Sjövall, H. & Hansson, G.C. 2010a. Bacteria

 

penetrate the inner mucus layer before inflammation in the dextran sulphate colitis model. *PLoS ONE* **5**, e12238.

Johansson, M.E., Larsson, J.M. & Hansson, G.C. 2010b. The two mucus layers of colon are organized by the MUC2 mucin, whereas the outer layer is a legislator of host-microbial interactions. *Proc Natl Acad Sci USA* **108** (Suppl 1), 4659–4665.

Juric, M., Xiao, F., Amasheh, S., May, O., Wahl, K., Bantel, H., Manns, M.P., Seidler, U. & Bachmann, O. 2013. Increased epithelial permeability is the primary cause for bicarbonate loss in inflamed murine colon. *Inflamm Bowel Dis* **19**, 904–911.

Kaunitz, J.D. & Akiba, Y. 2001. Duodenal intracellular bicarbonate and the 'CF paradox'. *JOP* **2**(Suppl 4), 268–273.

Kleessen, B., Kroesen, A.J., Buhr, H.J. & Blaut, M. 2002. Mucosal and invading bacteria in patients with inflammatory bowel disease compared with controls. *Scand J Gastroenterol* **37**, 1034–1041.

Lacy, E.R. 1988. Epithelial restitution in the gastrointestinal tract. *J Clin Gastroenterol* **10**(Suppl 1), S72–S77.

Lamprecht, G., Heil, A., Baisch, S., Lin-Wu, E., Yun, C.C., Kalbacher, H., Gregor, M. & Seidler, U. 2002. The down regulated in adenoma (dra) gene product binds to the second PDZ domain of the NHE3 kinase A regulatory protein (E3KARP), potentially linking intestinal $Cl^-/HCO3^-$ exchange to Na+/H+ exchange. *Biochemistry* **15**, 12336–12342.

Laubitz, D., Larmonier, C.B., Bai, A., Midura-Kiela, M.T., Lipko, M.A., Thurston, R.D., Kiela, P.R. & Ghishan, F.K. 2008. Colonic gene expression profile in NHE3-deficient mice: evidence for spontaneous distal colitis. *Am J Physiol Gastrointest Liver Physiol* **295**, G63–G77.

Laukoetter, M.G., Nava, P., Lee, W.Y., Severson, E.A., Capaldo, C.T., Babbin, B.A., Williams, I.R., Koval, M., Peatman, E., Campbell, J.A., Dermody, T.S., Nusrat, A. & Parkos, C.A. 2007. JAM-A regulates permeability and inflammation in the intestine in vivo. *J Exp Med* **204**, 3067–3076.

Lin, S., Yeruva, S., He, P., Singh, A.K., Zhang, H., Chen, M., Lamprecht, G., de Jonge, H.R., Tse, M., Donowitz, M., Hogema, B.M., Chun, J., Seidler, U. & Yun, C.C. 2010. Lysophosphatidic acid stimulates the intestinal brush border $Na^+/H^+$ exchanger 3 and fluid absorption via LPA5 and NHERF2. *Gastroenterology* **138**, 649–658.

Lochner, M., Ohnmacht, C., Presley, L., Bruhns, P., Si-Tahar, M., Sawa, S. & Eberl, G. 2011. Microbiota-induced tertiary lymphoid tissues aggravate inflammatory disease in the absence of RORgamma t and LTi cells. *J Exp Med* **208**, 125–134.

Musch, M.W., Wang, Y., Claud, E.C. & Chang, E.B. 2013. Lubiprostone decreases mouse colonic inner mucus layer thickness and alters intestinal microbiota. *Dig Dis Sci* **58**, 668–677.

Orlowski, J. 1993. Heterologous expression and functional properties of amiloride high affinity (NHE-1) and low affinity (NHE-3) isoforms of the rat Na/H exchanger. *J Biol Chem* **268**, 16369–16377.

Parmley, R.R. & Gendler, S.J. 1998. Cystic fibrosis mice lacking Muc1 have reduced amounts of intestinal mucus. *J Clin Invest* **102**, 1798–1806.

Petersson, J., Schreiber, O., Hansson, G.C., Gendler, S.J., Velcich, A., Lundberg, J.O., Roos, S., Holm, L. & Phillipson, M. 2011. Importance and regulation of the colonic mucus barrier in a mouse model of colitis. *Am J Physiol Gastrointest Liver Physiol* **300**, G327–G333.

Riegler, M., Feil, W., Wenzl, E. & Schiessel, R. 1991. Factors influencing the restitution of the duodenal and colonic mucosa after damage. *J Physiol Pharmacol* **42**, 61–71.

Schultheis, P.J., Clarke, L.L., Meneton, P., Miller, M.L., Soleimani, M., Gawenis, L.R., Riddle, T.M., Duffy, J.J., Doetschman, T., Wang, T., Giebisch, G., Aronson, P.S., Lorenz, J.N. & Shull, G.E. 1998. (1998) Renal and intestinal absorptive defects in mice lacking the NHE3 Na+/H+ exchanger. *Nat Genet* **19**, 282–285.

Schweinfest, C.W., Spyropoulos, D.D., Henderson, K.W., Kim, J.H., Chapman, J.M., Barone, S., Worrell, R.T., Wang, Z. & Soleimani, M. 2006. Slc26a3 (dra)-deficient mice display chloride-losing diarrhoea, enhanced colonic proliferation, and distinct up-regulation of ion transporters in the colon. *J Biol Chem* **281**, 37962–37971.

Singh, A.K., Riederer, B., Chen, M., Xiao, F., Krabbenhöft, A., Engelhardt, R., Nylander, O., Soleimani, M. & Seidler, U. 2010. The switch of intestinal Slc26 exchangers from anion absorptive to HCOFormula secretory mode is dependent on CFTR anion channel function. *Am J Physiol Cell Physiol* **298**, C1057–C1065.

Singh, A.K., Liu, Y., Riederer, B., Engelhardt, R., Thakur, B.K., Soleimani, M. & Seidler, U. 2013. Molecular transport machinery involved in orchestrating luminal acid-induced duodenal bicarbonate secretion in vivo. *J Physiol* **591**, 5377–5391.

Sørensen, M.V., Sausbier, M., Ruth, P., Seidler, U., Riederer, B., Praetorius, H.A. & Leipziger, J. 2010. Adrenaline-induced colonic $K^+$ secretion is mediated by KCa1.1 (BK) channels. *J Physiol* **588**, 1763–1777.

Swidsinski, A., Weber, J., Loening-Baucke, V., Hale, L.P. & Lochs, H. 2005. Spatial organization and composition of the mucosal flora in patients with inflammatory bowel disease. *J Clin Microbiol* **43**, 3380–3389.

Talbot, C. & Lytle, C. 2010. Segregation of $Na^+/H^+$ exchanger-3 and $Cl^-/HCO3^-$ exchanger SLC26A3 (DRA) in rodent caecum and colon. *Am J Physiol Gastrointest Liver Physiol* **299**, G358–G367.

Tuo, B., Riederer, B., Wang, Z., Colledge, W.H., Soleimani, M. & Seidler, U. 2006. Involvement of the anion exchanger SLC26A6 in prostaglandin E2- but not forskolin-stimulated duodenal $HCO_3^-$ secretion. *Gastroenterology* **130**, 349–358.

Van der Sluis, M., De Koning, B.A., De Bruijn, A.C., Velcich, A., Meijerink, J.P., Van Goudoever, J.B., Büller, H.A., Dekker, J., Van Seuningen, I., Renes, I.B. & Einerhand, A.W. 2006. Muc2-deficient mice spontaneously develop colitis, indicating that MUC2 is critical for colonic protection. *Gastroenterol* **131**, 117–129.

Walker, N.M., Simpson, J.E., Yen, P.F., Gill, R.K., Rigsby, E.V., Brazill, J.M., Dudeja, P.K., Schweinfest, C.W. & Clarke, L.L. 2008. Down-regulated in adenoma $Cl/HCO_3$ exchanger couples with Na/H exchanger 3 for NaCl absorption in murine small intestine. *Gastroenterology* **135**, 1645–1653.

  doi: 10.1111/apha.12220

Walker, N.M., Simpson, J.E., Brazill, J.M., Gill, R.K., Dudeja, P.K., Schweinfest, C.W. & Clarke, L.L. 2009. Role of down-regulated in adenoma anion exchanger in $HCO_3^-$ secretion across murine duodenum. *Gastroenterology* **136**, 893–901.

Wedenoja, S., Hoglund, P. & Holmberg, C. 2010. Review article: the clinical management of congenital chloride diarrhoea. *Aliment Pharmacol Ther* **31**, 477–485.

Wedenoja, S., Pekansaari, E., Höglund, P., Mäkelä, S., Holmberg, C. & Kere, J. 2011. Update on SLC26A3 mutations in congenital chloride diarrhoea. *Hum Mutat* **32**, 715–722.

Xia, W., Yu, Q., Riederer, B., Singh, A.K., Engelhardt, R., Yeruva, S., Song, P., Tian, D.A., Soleimani, M. & Seidler, U. 2013. The distinct roles of anion transporters Slc26a3 (DRA) and Slc26a6 (PAT-1) in fluid and electrolyte absorption in the murine small intestine. *Pflugers Arch*. Nov 14. [Epub ahead of print] DOI 10.1007/s00424-013-1381-2

Xiao, F., Juric, M., Li, J., Riederer, B., Yeruva, S., Singh, A.K., Zheng, L., Glage, S., Kollias, G., Dudeja, P., Tian, D.A., Xu, G., Zhu, J., Bachmann, O. & Seidler, U. 2012a. Loss of downregulated in adenoma (DRA) impairs mucosal $HCO_3^-$ secretion in murine ileocolonic inflammation. *Inflamm Bowel Dis* **18**, 101–111.

Xiao, F., Li, J., Singh, A.K., Riederer, B., Wang, J., Sultan, A., Park, H., Lee, M.G., Lamprecht, G., Scholte, B.J., De Jonge, H.R. & Seidler, U. 2012b. Rescue of epithelia $HCO_3^-$ secretion in murine intestine by apical membrane expression of the cystic fibrosis transmembrane conductance regulator mutant F508del. *J Physiol* **590**, 5317–5334.

Yang, N., Garcia, M.A. & Quinton, P.M. 2013. Normal Mucus Formation Requires cAMP-dependent $HCO_3^-$ Secretion and $Ca_2^+$-mediated Mucin Exocytosis. *J Physiol* **591**(Pt 18), 4581–4593.

## Supporting Information

Additional Supporting Information may be found in the online version of this article:

**Data S1.** Materials and methods.

**Table S1.** Acid/base parameters in the blood of Slc26a3$^{+/+}$ and Slc26a3$^{-/-}$ mice before surgery.

**Table S2.** Buffer compositions for the pHi measurements shown in Figures 4, 5 and S2) (in mM)

**Figure S1.** Histological and functional effects of acute DSS colitis induction by standard 7-day protocol in Slc26a3$^{+/+}$ mice.

**Figure S2.** Representative pHi trace of a single experiment to determine NHE3 transport activity.

**Figure S3.** Muc2 immunostaining and DAPI stain for the detection of nuclei and bacteria in the mid-distal colonic mucosa of slc9a3$^{-/-}$ (NHE3-deficient) mice.

**Figure S4.** PAS-Alcian Blue staining of mid-distal colon of Slc26a3-deficient and WT mice after the DSS treatment.

 